



Published in final edited form as:

*J Magn Reson Imaging*. 2013 April ; 37(4): 778–790. doi:10.1002/jmri.23834.

## Clinical and Technical Considerations for High Quality Breast MRI at 3 Tesla

Habib Rahbar, MD\*, Savannah C. Partridge, PhD, Wendy B. DeMartini, MD, Bonnie Thursten, BSRT(R)MR, and Constance D. Lehman, MD, PhD

Department of Radiology, University of Washington, Seattle Cancer Care Alliance, Seattle, Washington, USA.

### Abstract

The use of breast MRI at 3 tesla (T) has increased in use substantially in recent years. Potential benefits of moving to higher field strength MRI include improved morphologic and kinetic assessment of breast lesions through higher spatial and temporal resolution dynamic contrast-enhanced MR examinations. Furthermore, higher field strength holds promise for the development of superior advanced breast MRI techniques, such as diffusion weighted imaging and MR spectroscopy. To fully realize the benefits of moving to 3T, a thorough understanding of the technical and safety challenges of higher field strength imaging specific to breast MRI is paramount. Through the use of advanced coil technology, parallel imaging, dual-source parallel radiofrequency excitation, and image-based shimming techniques, many of these limiting technical factors can be overcome to achieve high quality breast MRI at 3T.

### Keywords

breast MRI; 3 Tesla; review; technical

---

THE MOVE TO higher magnetic field strength holds promise for improving the quality of magnetic resonance imaging (MRI) of the breast. The potential advantages include improved spatial resolution, improved contrast, and decreased scan times. However, additional technical, physical, and safety challenges involved in imaging at higher field strength must be addressed to realize these advantages. The aim of this article is to discuss the clinical and technical considerations for the optimization of breast MRI protocols at 3 tesla (T).

### BACKGROUND: CLINICAL UTILITY OF BREAST MRI

MRI has become an important tool for breast cancer detection and characterization. Current evidence-based clinical applications of breast MRI include the evaluation of patients with a new diagnosis of breast cancer, screening high risk patients, monitoring response to neoadjuvant chemotherapy, assessment of silicone implant integrity, and the evaluation of patients with metastatic axillary adenocarcinoma of unknown primary (1). Conventional breast MRI protocols incorporate dynamic contrast-enhanced MRI (DCE MRI) series, with

---

\*Address reprint requests to: H.R., University of Washington School of Medicine, Seattle Cancer Care Alliance, 825 Eastlake Avenue E., G3-200, Seattle, WA 98109-1023. hrahbar@uw.edu.

interpretation of both morphologic and enhancement kinetic features as described in the standardized American College of Radiology Breast Imaging-Reporting and Data System (BI-RADS) MRI lexicon (2).

## INCREASED SIGNAL TO NOISE RATIO AT 3T

Perhaps the greatest appeal of breast imaging at 3T over 1.5T is the potential doubling of signal to noise ratio (SNR), as suggested by the linear relationship of SNR to magnetic field strength ( $B_0$ ) for a spoiled gradient echo sequence (3):

$$SNR \propto B_0 V \sqrt{\frac{\text{measurements}}{BW}} \frac{\left( \sin(\theta) \left( 1 - e^{-\frac{-TR}{T1}} \right) \right)}{\left( 1 - e^{-\frac{-TR}{T1}} \cos(\theta) \right)} e^{-\frac{-TE}{T2}}$$

Where  $V$  = voxel volume, measurements = number of acquired phase encode lines  $\times$  number of acquired partitions  $\times$  number of signals averaged,  $HW$  = receiver bandwidth per pixel,  $T1$  = longitudinal relaxation time, and  $T2$  = transverse relaxation time, and  $\theta$  = flip angle. However, in practice a true doubling of SNR does not occur at 3T for clinical imaging due to the effects of longer  $T1$  relaxation times and adjustments to limit specific absorption rate (SAR) deposition at higher magnetic field strength. Nonetheless, imaging at 3T does provide a significant increase in SNR over 1.5T, by a factor of approximately 1.6 to 1.7 for gradient echo-based  $T1$ -weighted sequences (3), and this higher SNR can be thought of as currency that can be used to improve certain facets of a breast MR examination. It should also be noted that gains in SNR related to greater magnetic field strength are also dependent on breast coil quality. Coils that use a greater coil count with smaller elements and provide a close anatomic fit are known to provide a significant SNR benefit (4).

## POTENTIAL CLINICAL ADVANTAGES AT 3T

High quality breast MRI depends on the ability of the radiologist to identify and accurately characterize lesions. At higher field strength, improved lesion detection may be achieved through gains in spatial resolution, more homogeneous fat suppression, and greater contrast-to-noise ratio (CNR), while lesion characterization may be improved through higher spatial and/or temporal resolution. Potential clinical advantages are summarized in Table 1.

### Spatial Resolution

The ability to discern anatomical detail can be improved at 3T by exchanging increased SNR for improved spatial resolution. Improved anatomic detail improves the ability to assess tissue architecture, identify abnormalities, and assess involvement of the pectoralis muscle, chest wall, skin, and nipple-areola complex. An example of superior anatomic detail achieved at 3T over 1.5T is provided in Figure 1. Furthermore, maximum intensity projection images (MIPs) at higher spatial resolution can demonstrate greater detail, also

aiding in lesion detection and characterization of normal physiological background enhancement versus malignant processes, Figure 2.

Improved morphological detail can impact assessment of lesions identified on breast MRI. In the only published study to date comparing the intra-patient diagnostic performance of 3T breast MRI to 1.5T, Kuhl et al demonstrated a higher diagnostic confidence in the evaluation of breast lesions at 3T, specifically noting the improved ability to resolve dark internal septations characteristic of fibroadenomata (5). Many morphological details, such as spiculations, are on the order of 1 mm in size (6); as a result, imaging with high spatial resolution less than 1 mm at 3T is critical for realization of improved morphological detail (6). In our experience at the University of Washington, we have also observed a greater ability to define morphological features such as fine spiculations (Fig. 3) and dark internal septations (Fig. 4) due to the increased spatial resolution achievable at 3T compared with 1.5T.

### Temporal Resolution

Lesion kinetics assessments can also be improved at higher field strength by translating higher SNR into improved temporal resolution for more detailed enhancement information. Typically, invasive breast cancers demonstrate early phase enhancement with subsequent delayed phase washout. Prior studies have demonstrated that this initial rapid enhancement occurs within 60 to 120 s after injection (6). However, kinetic behavior depends on several factors, including histology, lesion grade, and microvessel density (7–9) resulting in a spectrum of enhancement curves for breast lesions with varying initial enhancement and delayed washout rates. Higher temporal resolution may enhance the accuracy of breast lesions' kinetics profiles. Furthermore, increased temporal resolution enables pharmacokinetic analysis; these quantitative measures can provide potentially more valuable information for lesion characterization and monitoring of treatment response (10,11). Typically, achievable temporal resolution is limited by spatial resolution goals. However, new “hybrid” approaches to DCE MRI breast acquisition hold potential for minimizing the temporal-spatial resolution trade-offs for breast imaging at 3T (12). Such an approach uses increased parallel imaging factors, facilitated by SNR gains at 3T, to combine high spatial and temporal resolution acquisitions in a single MR sequence.

### Fat Suppression

Improved fat suppression is another potential advantage of imaging at 3T due to greater spectral separation of fat and water at higher field strength (Fig. 5). This improved fat suppression helps ensure that lesions are not obscured by bright fat signal due to incomplete or poor fat suppression and thus can aid in lesion detection. An example of improved fat suppression at 3T over 1.5T in the same patient is demonstrated in Figure 6. However, there are challenges to realizing this advantage due to increased  $B_0$  and  $B_1$  (applied radiofrequency magnetic field) variations at 3T, which can affect fat suppression uniformity (Fig. 7). As a result, achieving good quality fat suppression requires techniques to reduce  $B_0$  and  $B_1$  inhomogeneities (e.g. higher order shimming and multi-source parallel RF excitation, described in more detail below) and/or use of fat suppression approaches that are

insensitive to  $B_1$  field variations, such as those that incorporate adiabatic frequency-selective inversion pulses.

### Contrast-to-Noise Ratio

Lastly, lesion detection is dependent on achieving a high contrast-to-noise ratio (CNR), which is impacted by field strength effects on T1 relaxation times of breast tissue and gadolinium. At 3T, the T1 relaxation time is increased for both fat and glandular tissue in the breast by approximately 21% and 17% respectively, but T1 relaxation of gadolinium is increased to a much lesser extent (13). This suggests that the relative difference in signal intensity between enhancing lesions and nonenhancing tissues would be increased at 3T, thus making enhancing lesions more conspicuous. However, it is currently unclear whether such T1 relaxation time effects impact benign background parenchymal enhancement, which could also affect lesion conspicuity.

## TECHNICAL CONSIDERATIONS

While breast MRI at 3T holds potential advantages over 1.5T, there are technical challenges that must be addressed. Parallel imaging is a key factor in realizing the benefits of 3T MRI from a practical standpoint, requiring multi-channel radiofrequency (RF) coils. Additionally, potentially elevated energy deposition raises patient safety concerns, and elevated  $B_1$  and  $B_0$  inhomogeneities are particular obstacles for obtaining high quality images at 3T. Strategies to address these challenges are outlined below and are summarized in Table 2.

### Parallel Imaging

First and foremost, parallel imaging is critical for realizing the benefits of higher field strength breast MRI. While translating higher SNR to increased spatial or temporal resolution can be achieved with different techniques such as increased receiver bandwidth and noncartesian  $k$ -space sampling, the use of RF coils with a greater number of coil elements and increased parallel imaging capability is particularly efficient for breast imaging (4). By combining spatial sensitivities of multiple receiver coils in a phased array, parallel imaging reduces scan time. This can allow breast MR examinations to be obtained at faster rates while maintaining adequate resolution and coverage or scan length to be maintained while increasing the number of slices and pixels acquired to achieve higher spatial resolution. The number of coil elements as well as the layout affects the maximum acceleration factor  $R$  achievable in each orthogonal direction, which is particularly important for 3D acquisitions where parallel imaging can be used in multiple directions simultaneously (Fig. 8). Although acceleration factors are typically limited to 4 or less at 1.5T due to SNR limitations, a considerably higher  $R$  is possible at higher field strengths (14). Newer MRI systems available typically support up to 32 simultaneous RF channels (15). At present, 16-channel phased-array breast coils provide the highest potential acceleration factor for 3T breast imaging with commercially available hardware, but new higher channel coils are under development and are expected to further improve spatial resolution capabilities.

### Patient Safety: SAR concerns

SAR is roughly quadrupled at 3T compared with 1.5T if RF pulses and sequences are held constant. As a result, SAR induced temperature changes of a human body are a significant safety issue of high-field MRI. This potential high energy deposition is especially problematic in imaging sequences using many RF pulses in short time periods, such as fast spin-echo sequences (16). In general, SAR constraints have not posed a major issue for breast imaging at 3T; however, some tradeoffs in image acquisition rates, resolution, and slice coverage may be necessary to reduce power deposition.

A chief strategy for addressing SAR issues is using parallel imaging to reduce MR imaging times and resulting RF power deposition. This requires the use of multi-channel RF coils with a greater number of coil elements to increase the obtainable parallel imaging acceleration factor  $R$ . Additional strategies to mitigate SAR effects include alternate RF excitation pulse designs (such as lower peak-amplitude pulses) and modified sequence designs incorporating reduced flip angles (such as for refocusing pulses in fast spin-echo sequences), shorter echo train lengths, or longer repetition times (17). Usage of multi-source parallel RF excitation techniques (e.g., dual-source) (18,19) has also been reported to reduce SAR for body imaging applications at 3T; however, the amount of SAR reduction may vary from patient to patient and has not yet been assessed for breast imaging.

### $B_0$ Inhomogeneity

Accurate undistorted imaging with good quality fat suppression requires the magnetic field ( $B_0$ ) to be homogeneous throughout the entire region of interest. For breast MRI at 3T,  $B_0$  inhomogeneity can manifest as poor fat suppression (Fig. 9) and/or magnetic susceptibility effects. Magnetic susceptibility effects often occur at the interfaces between soft tissue (breast) and air as a result of  $B_0$  variations. Susceptibility artifacts scale linearly with increasing field strength and are, therefore, twice as prominent at 3T compared with 1.5T (17). Achieving adequate  $B_0$  homogeneity for breast imaging at 3T requires improved shimming techniques over 1.5T. New image-based higher order shimming methods can dramatically improve  $B_0$  homogeneity for bilateral breast imaging, Figure 10. Parallel imaging also reduces image artifacts and distortions caused by susceptibility effects associated with echo planar imaging by shortening echo train lengths.

### $B_1$ Inhomogeneity

Another technical issue associated with high-field imaging is spatial inhomogeneity of the applied radiofrequency magnetic field ( $B_1$ ). This results from standing wave and/or dielectric effects (caused by interaction between the coil and electromagnetic properties of the tissue being imaged), which are more pronounced at 3T due to the higher RF transmit frequency and shorter wavelength than at lower field strength (20). Breast imaging is particularly susceptible to  $B_1$  inhomogeneities due to the large FOV necessary for bilateral imaging and off-center positioning of the patient's torso within the transmitting whole-body RF birdcage coil giving rise to unequal loading effects (21).  $B_1$  inhomogeneities cause the applied flip angle and signal measured to be nonuniform across the field of view, which can result in a loss of tissue contrast, creating "shading" and decreased diagnostic power depending on location.

Potential approaches for mitigating this problem include using 3D imaging, which is less affected than 2D imaging due to inherently higher baseline T1 contrast from a much shorter TR (17). This issue can also be addressed by increasing the flip angle, but this incurs a significant SAR penalty, making it a less desirable approach. Recently, dual-source parallel RF excitation techniques have been developed, which can largely prevent B<sub>1</sub> inhomogeneities (18,19). Dualsource parallel RF excitation is an adaptive excitation technique that uses multiple transmit coils and is able to independently control the RF waveforms and compensate for patient-induced B<sub>1</sub> inhomogeneities (Fig. 11) (22). Parallel RF excitation can provide improved RF uniformity, improved consistency in image quality (contrast, signal homogeneity, and fat suppression), and reduced RF energy deposition (18,19,23).

## CONSIDERATIONS FOR ADVANCED BREAST MRI TECHNIQUES

There are several emerging advanced MRI techniques that are currently being investigated. The move to higher field strength provides opportunities for improvements in these techniques as well. An overview of some considerations related to diffusion weighted imaging (DWI) and MR spectroscopy (MRS) is provided below.

### Diffusion-Weighted Imaging

DWI is a non-contrast-enhanced technique that measures the ability of water molecules to freely diffuse and is sensitive to the microstructural properties of tissue. Numerous studies have shown DWI to be useful for differentiating carcinomas from normal breast tissue and benign lesions (24,25), raising the possibility of a noncontrast breast MRI technique for detection of mammographically occult breast cancer (e.g., Fig. 12). DWI has also shown potential to improve the positive predictive value of lesion characterization when used as an adjunct to the standard DCE breast MRI protocol (26). A major limitation inherent to DWI is limited SNR; thus it may be advantageous to perform DWI at higher field strength. Increases in SNR at 3T could help to improve CNR and spatial resolution, which could aid in the detection of smaller lesions. An example of improved spatial resolution in DWI at 3T compared with 1.5T is provided in Figure 13.

In theory, apparent diffusion coefficient (ADC) measures are independent of field strength, and thus previously reported thresholds for a given b value should remain unchanged. This was confirmed by an initial study directly comparing the visibility of lesions on DWI and their ADC values at 1.5 and 3T (27). The authors demonstrated that ADC values are not affected by increasing field strength, but smaller lesions (< 1 cm) were significantly more visible at 3T. While ADC values are not affected by field strength, the selected b values for DWI affects both CNR and ADC values. A recent study at 3T by Bogner et al has demonstrated that acquiring two b values in the range of 5 and 850 s/mm<sup>2</sup> is optimal for both ADC calculation and DW image quality (28).

Preliminary studies of DWI at 3T have shown promise for its use as a noncontrast technique for breast cancer detection and the improvement of standard DCE breast MRI accuracy. In a pilot study of 3T breast DWI, a total of 31 lesions were assessed with DCE MRI, qualitative DWI, and quantitative DWI; the authors achieved similar sensitivities for breast cancer

detection with the three methods (95%, 95%, and 90%, respectively) and found that quantitative DWI at 3T with predetermined ADC thresholds was equivalent in specificity (91%) to DCE MRI (29). Furthermore, El Khouli et al recently demonstrated that adding DWI to the standard 3T DCE imaging protocol has potential to improve the accuracy for breast lesion characterization (30).

### MR Spectroscopy

MRS is another non-contrast-enhanced technique that detects proton-containing metabolites. In the case of invasive breast malignancies, increased choline levels owing to increased cellularity and cell turnover have been reported with MRS. However, preinvasive cancers [i.e., ductal carcinoma in situ (DCIS)] and infiltrating breast cancers with a large DCIS component are often negative for elevated choline levels, somewhat limiting the sensitivity of this technique(31). While MRS measurement of breast tumor choline levels have been successfully performed on 1.5T MR scanners, higher field strength holds the potential to improve choline detectability, decrease measurement errors, and enable the assessment of smaller lesions through increases in both SNR and spectral resolution(32). An example of breast MRS obtained at 3T is shown in Figure 14.

One technical consideration for MRS at higher field strength is the need for more quantitative methods of choline detection, as at higher field strengths choline is detectable in normal breast tissue as well as in malignancies (33). It has recently been reported that due to this increased sensitivity for choline level detection at higher field strength, changes measured in breast tumor choline levels may be used as an early predictive marker of treatment response. In a preliminary study of patients undergoing neoadjuvant therapy, reduction of choline levels as early as 24 hours after the first dose of chemotherapy correlated with response as measured by final change in tumor size (34).

While to date most breast MRS approaches involve single voxel acquisitions that sample only a single region, 3D MR spectroscopic imaging (MRSI) has potential to greatly improve the clinical utility of breast MRS. 3D MRSI covers a large fraction of the breast, acquiring spectra for multiple voxels during a single acquisition. This 3D coverage simplifies voxel planning because it does not require prior localization of a lesion and allows the spectroscopy to be performed before injection of contrast. MRSI enables characterization of multi-focal or multi-centric lesions and direct comparison to normal breast tissue regions. In a recent article, Gruber et al have reported promising results implementing a quantitative 3D breast MRSI acquisition for differentiation of benign and malignant lesions (35).

## PRACTICAL IMPLEMENTATION OF A 3T BREAST MRI PROTOCOL

At the University of Washington, we have implemented a clinical 3T breast MRI protocol that provides high-quality dynamic contrast-enhanced breast MRI with higher spatial resolution than we are able to achieve at 1.5T. Smaller voxel sizes are acquired at 3T within the same scan time using higher parallel imaging factor, larger acquisition matrix, and smaller field of view. Differences between our 1.5T and 3T breast MRI protocols are summarized in Table 3. The 3T breast MRI images shown in Figures 1–10, 12, 13 were obtained using the University of Washington protocol. While our clinical breast DCE

protocol was designed with emphasis on spatial resolution, other institutions have implemented protocols with higher temporal resolution, such as the example from University of Chicago shown in Figure 15, protocol summarized in Table 3.

There are also several practical challenges to clinical breast imaging at higher field strength. Larger data sets due to increased spatial and/or temporal resolution necessitate increased data storage and handling capabilities for the scanner, as well as for offline computer-aided evaluation, data analysis, and picture archiving and communication systems (PACS). At this time, there is limited information regarding the effect of higher field strength on practical clinical image interpretation. With improvements in spatial and contrast resolution, it will be important to reassess morphological predictors of malignancy (36). In addition, it is unclear whether 3T field strength affects benign background parenchymal enhancement and kinetic curves.

Performing MR imaging-guided breast biopsy at higher field strength may require small adjustments in imaging approach. As susceptibility artifact increases both with field strength and with needle size, there can be an increase in the signal void of biopsy devices at 3T. Peters et al reported a signal void that was over twice the size of that at 1.5T for a 14-gauge core needle; however, there was no appreciable effect on diagnostic accuracy of the biopsy specimens obtained (37). If deemed necessary, alterations to the imaging protocol such as increasing bandwidth or reducing echo time may help to minimize susceptibility artifacts and reduce the signal void of a biopsy device at 3T. Alternatively, in our approach of using a plastic obturator during biopsy scans, we have noted the reverse problem in that the high degree of fat suppression at 3T made it more difficult to discern the location of the tip of the obturator (i.e., the center of the biopsy chamber for a vacuum-assisted breast biopsy device). Our solution was to decrease the level of fat suppression for the MR-guided biopsy scans by altering the SPAIR (spectral attenuated inversion recovery) delay to achieve less than maximal fat signal suppression, Figure 16.

## CONCLUSION

Transitioning from 1.5T to 3T for clinical breast MRI presents both exciting opportunities and technical challenges. Perhaps most importantly, scanning at 3T can provide breast MR images with higher spatial and temporal resolution. However, these improvements can be realized only through optimization of a variety of technical factors including use of a multi-channel breast coil, parallel RF transmission, and high order shimming. Without addressing the multiple technical factors, imaging at 3T can yield images that are inferior in quality to that of lower field strengths. In our experience, achieving high quality breast MR imaging at 3T requires a significant investment in protocol development for successful implementation. In the future, clinical studies will elucidate whether the technical advantages and image quality improvement afforded by breast MRI at 3T will have significant clinical impact.

## ACKNOWLEDGMENTS

The authors wish to acknowledge Hiroyuki Abe, MD, PhD (University of Chicago), Patrick Bolan, PhD (University of Minnesota), and Mark Rosen, MD, PhD (University of Pennsylvania) for their contributions to figure examples. We also thank Yvonne Rijckaert of Philips Healthcare for her technical assistance in developing our 3T breast MRI



program. This manuscript was adapted from an electronic educational poster (#4635) presented at 2011 ISMRM meeting in Montreal, Canada, entitled "Optimizing Breast Magnetic Resonance Imaging at 3.0 T."

## REFERENCES

1. DeMartini W, Lehman C, Partridge S. Breast MRI for cancer detection and characterization: a review of evidence-based clinical applications. *Acad Radiol* 2008;15:408–416. [PubMed: 18342764]
2. Ikeda DM, Hylton NM, Kuhl CK, et al. BI-RADS: magnetic resonance imaging, 1st edition. In: D'Orsi CJ, Mendelson EB, Ikeda DM, et al., editors. *Breast imaging reporting and data system: ACR BI-RADS - breast imaging atlas*. Reston, VA: American College of Radiology; 2003 p 111–113.
3. Merkle EM, Dale BM. Abdominal MRI at 3.0 T: the basics revisited. *AJRAm J Roentgenol* 2006;186:1524–1532.
4. Nnewiwe AN, Grafendorfer T, Daniel BL, et al. Custom-fitted 16-channel bilateral breast coil for bidirectional parallel imaging. *Magn Reson Med* 2011;66:281–289. [PubMed: 21287593]
5. Kuhl CK, Jost P, Morakkabati N, Zivanovic O, Schild HH, Gieseke J. Contrast-enhanced MR imaging of the breast at 3.0 and 1.5 T in the same patients: initial experience. *Radiology* 2006;239:666–676. [PubMed: 16549623]
6. Kuhl CK. Breast MR imaging at 3T. *Magn Reson Imaging Clin N Am* 2007;15:315–320, vi. [PubMed: 17893052]
7. Esserman L, Hylton N, George T, Weidner N. Contrast-enhanced magnetic resonance imaging to assess tumor histopathology and angiogenesis in breast carcinoma. *Breast J* 1999;5:13–21. [PubMed: 11348250]
8. Knopp MV, Weiss E, Sinn HP, et al. Pathophysiologic basis of contrast enhancement in breast tumors. *J Magn Reson Imaging* 1999;10:260–266. [PubMed: 10508285]
9. Hylton N. Dynamic contrast-enhanced magnetic resonance imaging as an imaging biomarker. *J Clin Oncol* 2006;24:3293–3298. [PubMed: 16829653]
10. Huang W, Tudorica LA, Li X, et al. Discrimination of benign and malignant breast lesions by using shutter-speed dynamic contrast-enhanced MR imaging. *Radiology* 2011;261:394–403. [PubMed: 21828189]
11. Li X, Huang W, Yankeelov TE, Tudorica A, Rooney WD, Springer CS, Jr. Shutter-speed analysis of contrast reagent bolus-tracking data: preliminary observations in benign and malignant breast disease. *Magn Reson Med* 2005;53:724–729. [PubMed: 15723402]
12. Pinker K, Grabner G, Bogner W, et al. A combined high temporal and high spatial resolution 3 Tesla MR imaging protocol for the assessment of breast lesions: initial results. *Invest Radiol* 2009;44:553–558. [PubMed: 19652611]
13. Rakow-Penner R, Daniel B, Yu H, Sawyer-Glover A, Glover GH. Relaxation times of breast tissue at 1.5T and 3T measured using IDEAL. *J Magn Reson Imaging* 2006;23:87–91. [PubMed: 16315211]
14. Wiesinger F, Van de Moortele PF, Adriany G, De Zanche N, Ugurbil K, Pruessmann KP. Potential and feasibility of parallel MRI at high field. *NMR Biomed* 2006;19:368–378. [PubMed: 16705638]
15. Ladd ME. High-field-strength magnetic resonance: potential and limits. *Top Magn Reson Imaging* 2007;18:139–152. [PubMed: 17621228]
16. Boss A, Graf H, Berger A, et al. Tissue warming and regulatory responses induced by radio frequency energy deposition on a whole-body 3-Tesla magnetic resonance imager. *J Magn Reson Imaging* 2007;26:1334–1339. [PubMed: 17969173]
17. Rakow-Penner R, Hargreaves B, Glover GH, Daniel B. Breast MRI at 3T. *Appl Radiol* 2009;38:6–13.
18. Nelles M, Konig RS, Gieseke J, et al. Dual-source parallel RF transmission for clinical MR imaging of the spine at 3.0 T: intraindividual comparison with conventional single-source transmission. *Radiology* 2010;257:743–753. [PubMed: 20858848]

19. Willinek WA, Gieseke J, Kukuk GM, et al. Dual-source parallel radiofrequency excitation body MR imaging compared with standard MR imaging at 3.0 T: initial clinical experience. *Radiology* 2010;256:966–975. [PubMed: 20720078]
20. Chang KJ, Kamel IR. Body MR imaging at 3T: basic considerations about artifacts and safety. In: Kamel IR, Merkle EM, editors. *Body MR imaging at 3 Tesla*. Cambridge: Cambridge University Press; 2011 p 1–11.
21. Azlan CA, Di Giovanni P, Ahearn TS, Semple SI, Gilbert FJ, Redpath TW. B1 transmission-field inhomogeneity and enhancement ratio errors in dynamic contrast-enhanced MRI (DCE-MRI) of the breast at 3T. *J Magn Reson Imaging* 2010;31:234–239. [PubMed: 20027594]
22. Partridge SC, Rahbar H, Lehman CD. Breast MR imaging In: Kamel IR, Merkle EM, editors. *Body MR imaging at 3 Tesla*. Cambridge: Cambridge University Press; 2011 p. 26–33.
23. Rahbar H, Partridge SC, Demartini WB, Gutierrez RL, Parsian S, Lehman CD. Improved B(1) homogeneity of 3 tesla breast MRI using dual-source parallel radiofrequency excitation. *J Magn Reson Imaging* 2012;35:1222–1226. [PubMed: 22282269]
24. Guo Y, Cai YQ, Cai ZL, et al. Differentiation of clinically benign and malignant breast lesions using diffusion-weighted imaging. *J Magn Reson Imaging* 2002;16:172–178. [PubMed: 12203765]
25. Woodhams R, Matsunaga K, Kan S, et al. ADC mapping of benign and malignant breast tumors. *Magn Reson Med Sci* 2005;4: 35<sup>2</sup>. [PubMed: 16127252]
26. Partridge SC, DeMartini WB, Kurland BF, Eby PR, White SW, Lehman CD. Quantitative diffusion-weighted imaging as an adjunct to conventional breast MRI for improved positive predictive value. *AJR Am J Roentgenol* 2009;193:1716–1722. [PubMed: 19933670]
27. Matsuoka A, Minato M, Harada M, et al. Comparison of 3.0-and 1.5-tesla diffusion-weighted imaging in the visibility of breast cancer. *Radiat Med* 2008;26:15–20. [PubMed: 18236129]
28. Bogner W, Gruber S, Pinker K, et al. Diffusion-weighted MR for differentiation of breast lesions at 3.0 T: how does selection of diffusion protocols affect diagnosis? *Radiology* 2009;253:341–351. [PubMed: 19703869]
29. Lo GG, Ai V, Chan JK, et al. Diffusion-weighted magnetic resonance imaging of breast lesions: first experiences at 3 T. *J Comput Assist Tomogr* 2009;33:63–69.
30. El Khouli RH, Jacobs MA, Mezban SD, et al. Diffusion-weighted imaging improves the diagnostic accuracy of conventional 3.0-T breast MR imaging. *Radiology* 2010;256:64–73. [PubMed: 20574085]
31. Sinha S, Sinha U. Recent advances in breast MRI and MRS. *NMR Biomed* 2009;22:3–16. [PubMed: 18654998]
32. Haddadin IS, McIntosh A, Meisamy S, et al. Metabolite quantification and high-field MRS in breast cancer. *NMR Biomed* 2009; 22:65–76. [PubMed: 17957820]
33. Meisamy S, Bolan PJ, Baker EH, et al. Adding in vivo quantitative <sup>1</sup>H MR spectroscopy to improve diagnostic accuracy of breast MR imaging: preliminary results of observer performance study at 4.0 T. *Radiology* 2005;236:465–475. [PubMed: 16040903]
34. Meisamy S, Bolan PJ, Baker EH, et al. Neoadjuvant chemotherapy of locally advanced breast cancer: predicting response with in vivo (<sup>1</sup>H) MR spectroscopy—a pilot study at 4 T. *Radiology* 2004;233:424–431. [PubMed: 15516615]
35. Gruber S, Debski BK, Pinker K, et al. Three-dimensional proton MR spectroscopic imaging at 3 T for the differentiation of benign and malignant breast lesions. *Radiology* 2011;261:752–761. [PubMed: 21998046]
36. Pinker-Domenig K, Bogner W, Gruber S, et al. High resolution MRI of the breast at 3 T: which BI-RADS(R) descriptors are most strongly associated with the diagnosis of breast cancer? *Eur Radiol* 2012;22:322–330. [PubMed: 21913060]
37. Peters NH, Meeuwis C, Bakker CJ, et al. Feasibility of MRI-guided large-core-needle biopsy of suspicious breast lesions at 3 T. *Eur Radiol* 2009;19:1639–1644. [PubMed: 19214520]

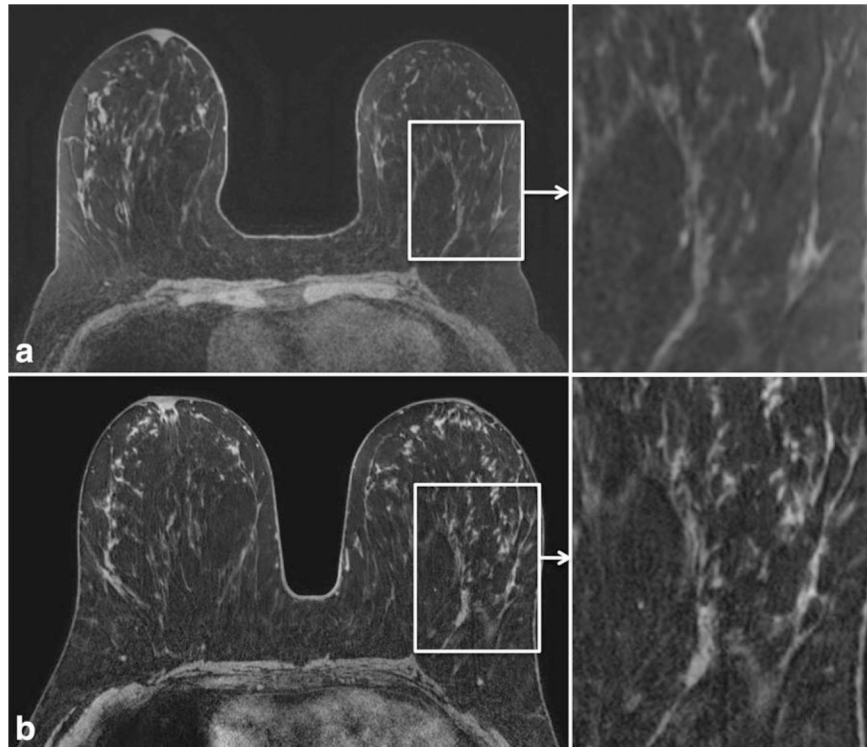


**Figure 1.** Comparison of the anatomical detail on dynamic contrast enhanced (DCE) breast MRI at 1.5T (**a**) and 3T (**b**) in the same patient. Improved spatial resolution was achieved at 3T (0.5 mm in-plane, 1.3 mm thick) compared with 1.5T (0.9 mm in-plane, 1.6 mm thick) within the same scan time of 3 minutes. Detailed scan parameters for breast MRI at 1.5T and 3T at the University of Washington are summarized in Table 3.

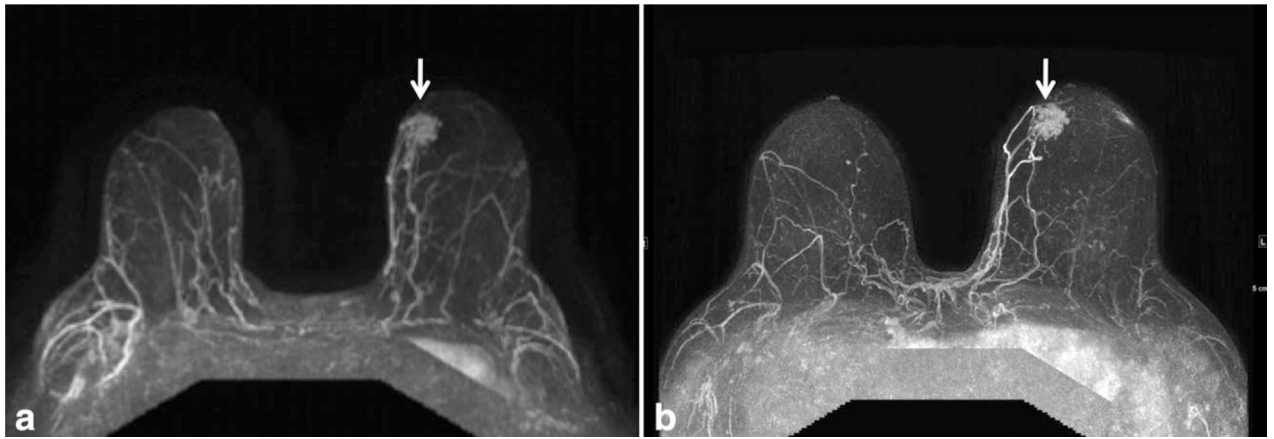


**Figure 2.** Improved maximum intensity projection images (MIP) in the same patient with newly diagnosed DCIS (arrows) without additional sites of suspicious enhancement on MRI performed at 1.5T (**a**) or 3T (**b**). Note the superior overall image quality of the 3T MIP providing improved definition of the breast vasculature, physiologic background enhancement, and the morphological features of the irregular mass (arrows). Detailed scan parameters for breast MRI at 1.5T and 3T at the University of Washington are summarized in Table 3.

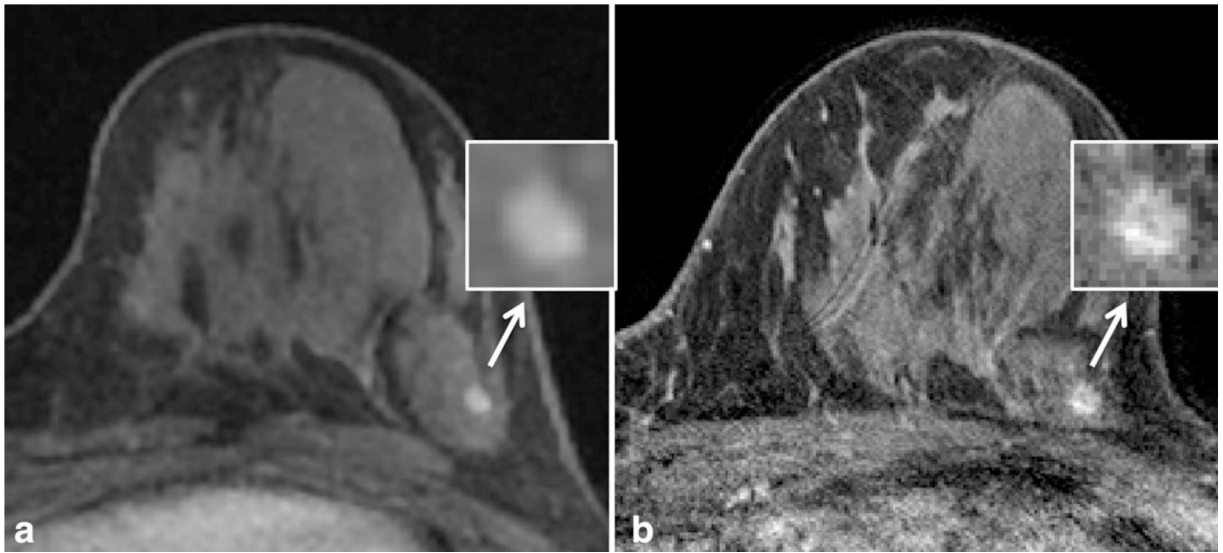


**Figure 3.**

Example of improved spatial resolution from dynamic contrast enhanced MRI at 1.5T (**a**) to 3T (**b**) leading to a change in lesion classification in a high-risk patient. At 1.5T, the lesion was described as a 4 mm oval circumscribed mass (arrow) with smooth margins (inset), probably benign (BI-RADS category 3). At 3T, the margins demonstrated fine spiculations (inset), and the mass was re-categorized as suspicious (BI-RADS category 4). MR guided biopsy yielded invasive ductal carcinoma. Detailed scan parameters for breast MRI at 1.5T and 3T at the University of Washington are summarized in Table 3.

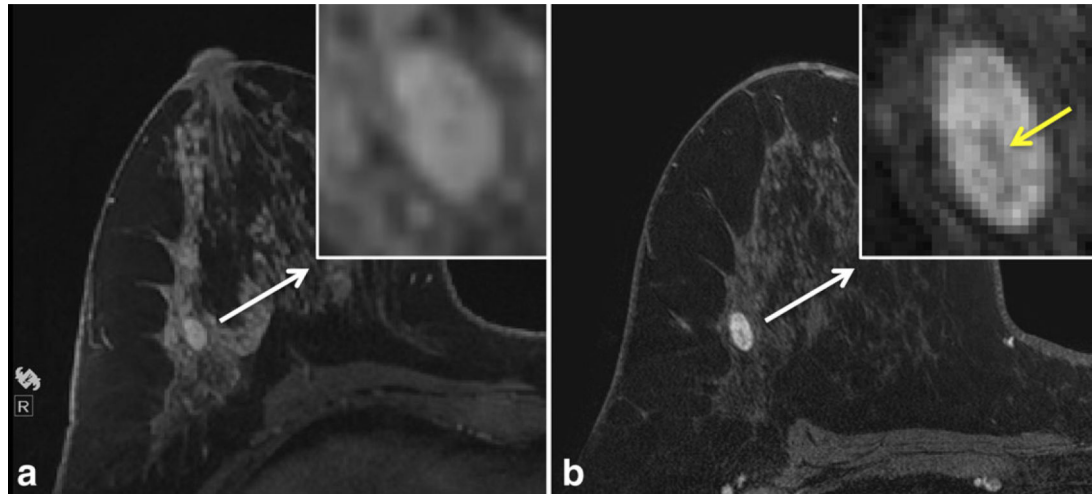


**Figure 4.**

Comparison of the imaging appearance at different field strengths of a biopsy-proven fibroadenoma in a high-risk patient. Dynamic contrast enhanced (DCE) MRI at 1.5T (**a**) demonstrates an oval shaped mass measuring 10 mm in size with smooth margins (inset). Scan obtained at 3T (**b**) demonstrates a dark internal septation (yellow arrow, inset) within the oval mass that was not previously resolved at 1.5T, a specific finding of fibroadenomata. Detailed scan parameters for breast MRI at 1.5T and 3T at the University of Washington are summarized in Table 3.

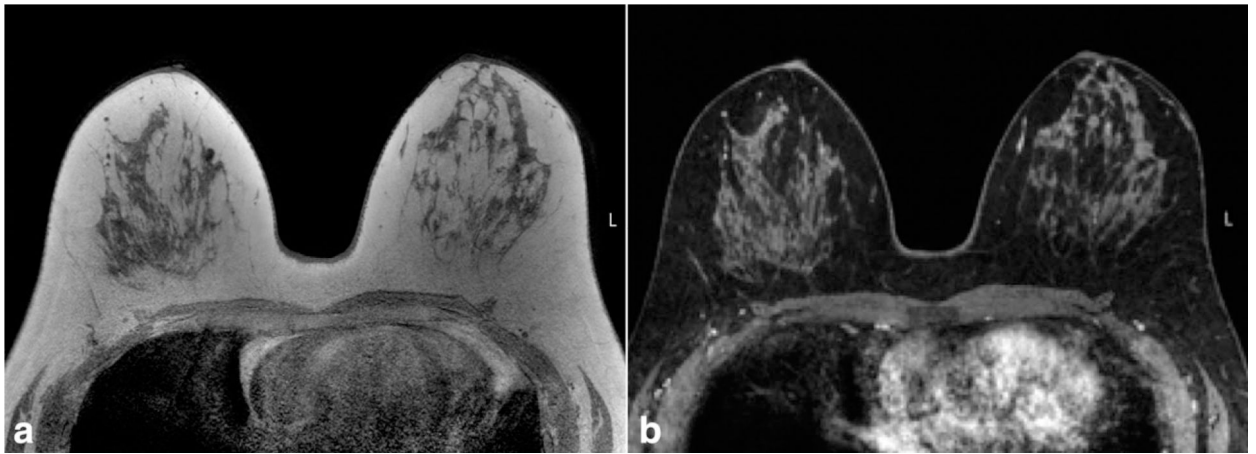


**Figure 5.** T1 precontrast image without fat suppression (**a**) and corresponding T1 postcontrast image with SPAIR fat suppression (**b**) obtained at 3T demonstrating uniform good quality fat suppression, which can aid in lesion detection.

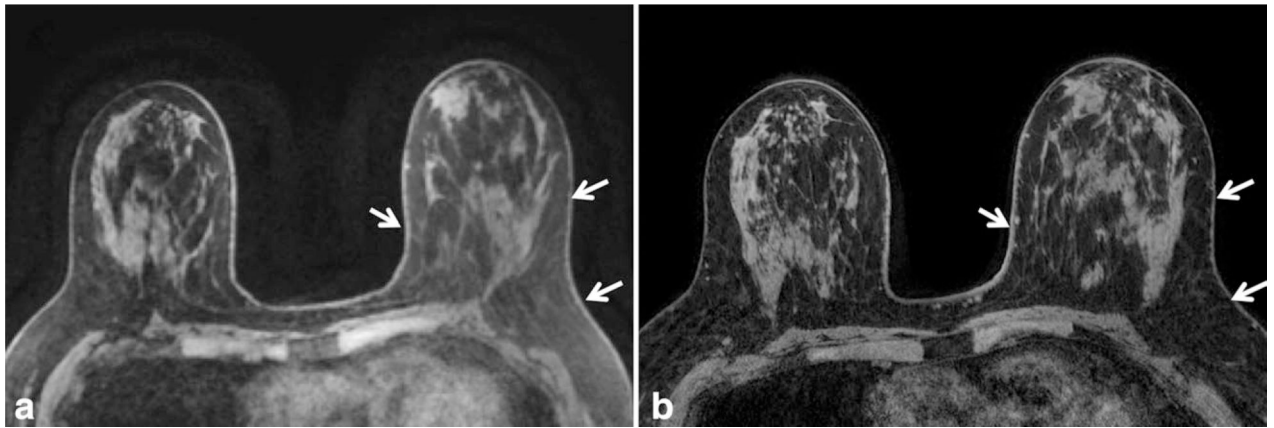


**Figure 6.** Comparison of quality of fat suppression in the same patient at 1.5T (**a**) and 3.0T (**b**). Note more homogeneous fat suppression is achieved using higher field strength on the T1-weighted precontrast fat suppressed images, particularly throughout the left breast (arrows).



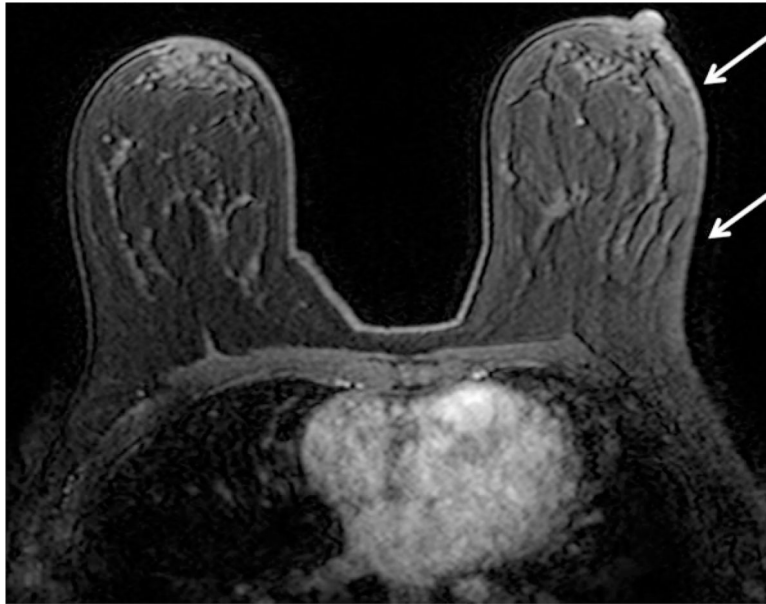


**Figure 7.** Example of  $B_1$  inhomogeneity manifesting as poor fat suppression on 3T breast MRI affecting the left breast (arrows) greater than the right breast. Poor fat suppression can compromise the ability of a radiologist to identify and characterize breast lesions.  $B_1$  inhomogeneities largely can be addressed with multi-source parallel RF excitation techniques.

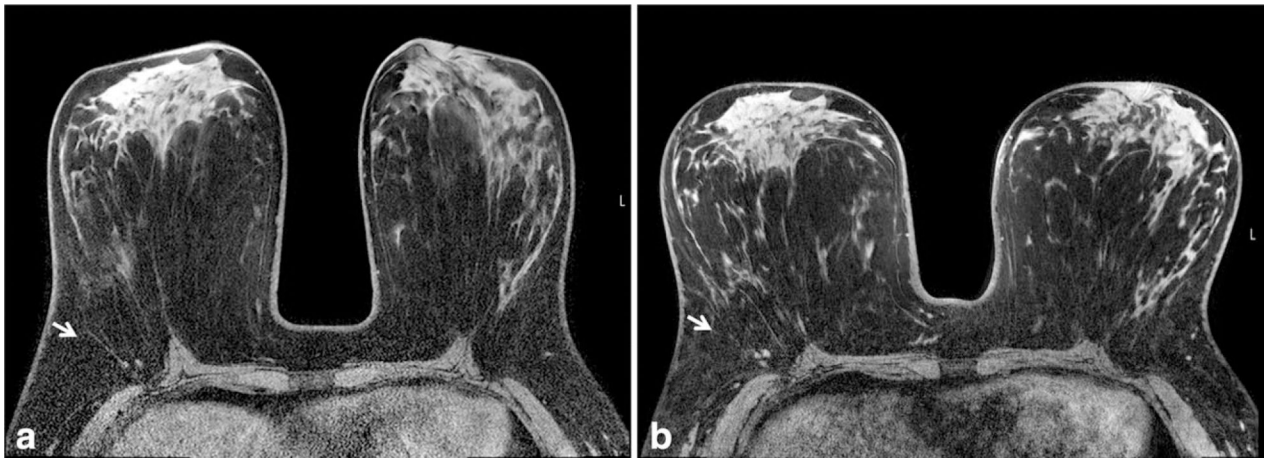


**Figure 8.**

Comparison of breast MR images acquired at 3T using 7-channel (a) and 16 channel (b) RF breast coils (both, Philips Healthcare, Best, the Netherlands). In both cases, imaging was performed using a 3D T1-weighted gradient echo sequence with parallel imaging and active fat suppression and scan time of 2:50 min. Higher spatial resolution was achieved within the same scan time using the 16-channel coil; acquired voxel sizes were  $0.5 \times 0.5 \times 1.3 \text{ mm}^3$  with the 16-channel coil (using parallel imaging in both the R/L and S/I directions) and  $0.7 \times 0.7 \times 1.5 \text{ mm}^3$  with the 7-channel coil (parallel imaging only possible in the R/L direction). Furthermore, the 16-channel coil provided increased SNR, particularly near the chest wall (arrows) compared with the 7-channel coil. From *Body MR Imaging at 3 Tesla*, edited by Ihab R. Kamel and Elmar M. Merkle. Copyright © 2011 Cambridge University Press. Reprinted with permission (22).



**Figure 9.** Example of  $B_0$  inhomogeneity manifesting as poor fat suppression on 3T breast MRI affecting both medial breasts (arrows) on T1-weighted images with fat suppression. Poor fat suppression can compromise the ability of a radiologist to identify and characterize breast lesions.  $B_0$  inhomogeneities largely can be addressed with image-based shimming techniques.

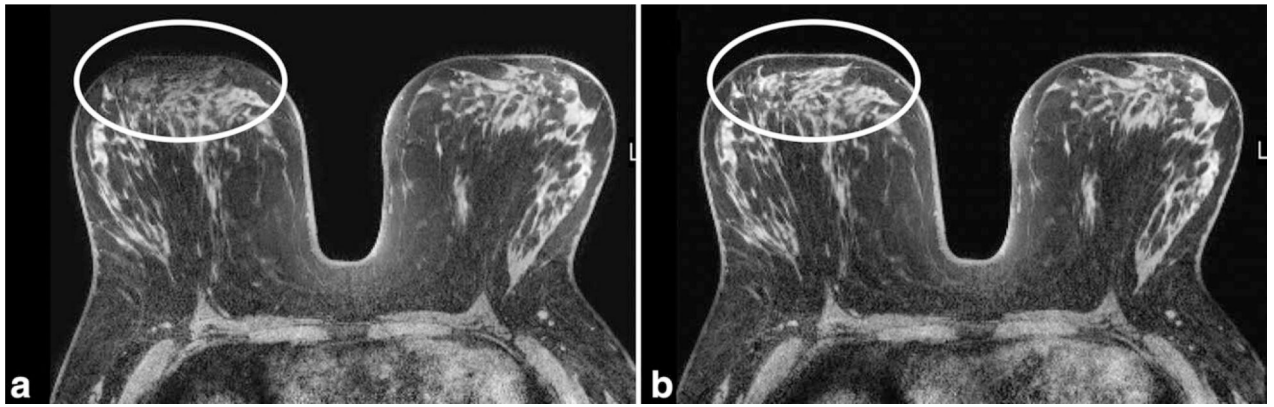


**Figure 10.**

The effect of different shimming techniques on  $B_0$  inhomogeneity on 3T breast MRI. Poor image quality is demonstrated at the air-tissue interfaces at the anterior aspect of the right breast (a) using standard rectangular volume shimming technique. Improved image quality at this location is achieved in the same patient by using “patient adaptive” image-based shimming (b). From *Body MR Imaging at 3 Tesla*, edited by Ihab R. Kamel and Elmar M. Merkle. Copyright © 2011 Cambridge University Press. Reprinted with permission (22).

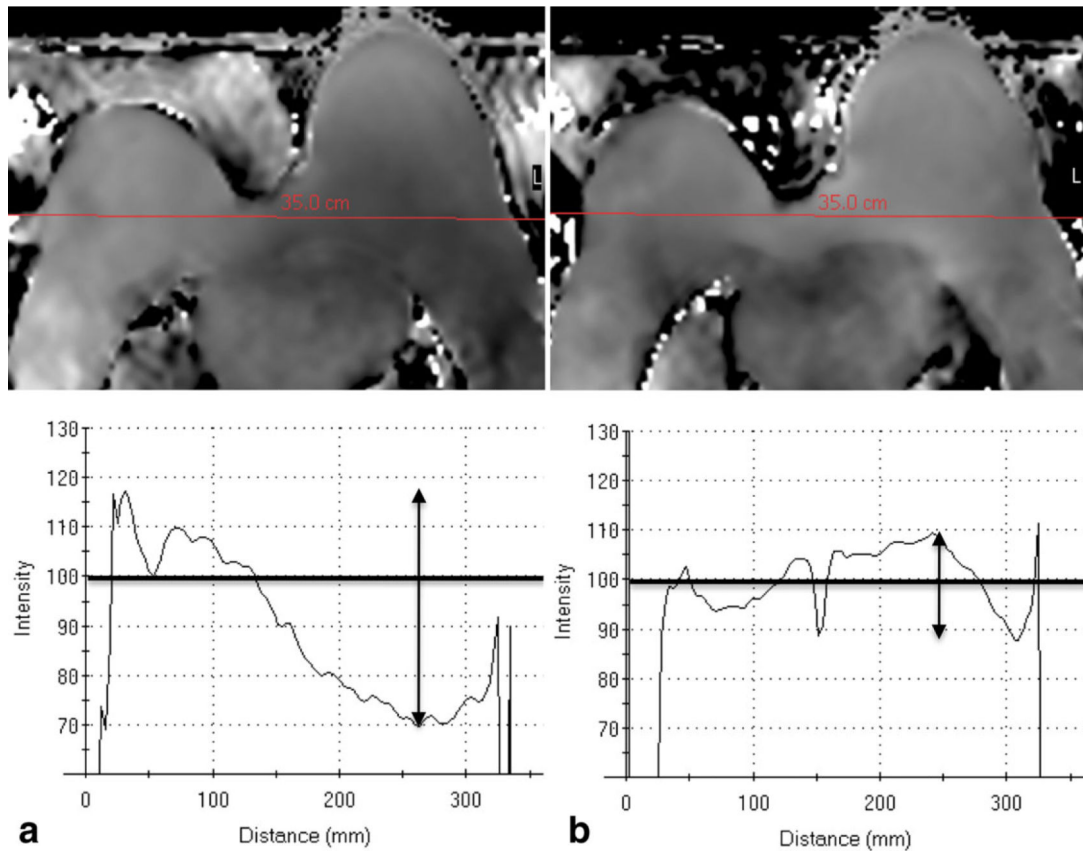


**Figure 11.**

B<sub>1</sub> inhomogeneity on breast MRI at 3T can largely be addressed using dual-source parallel RF excitation techniques. Using conventional single-source RF excitation technique (a), there is marked variation in B<sub>1</sub> intensity from right-to-left, with significant variations (arrows) from intended B<sub>1</sub> (100%). Dual-source parallel RF excitation technique (b) substantially improves B<sub>1</sub> inhomogeneity, creating more uniform right-to-left signal. From *Body MR Imaging at 3 Tesla*, edited by Ihab R. Kamel and Elmar M. Merkle. Copyright © 2011 Cambridge University Press. Reprinted with permission (22).

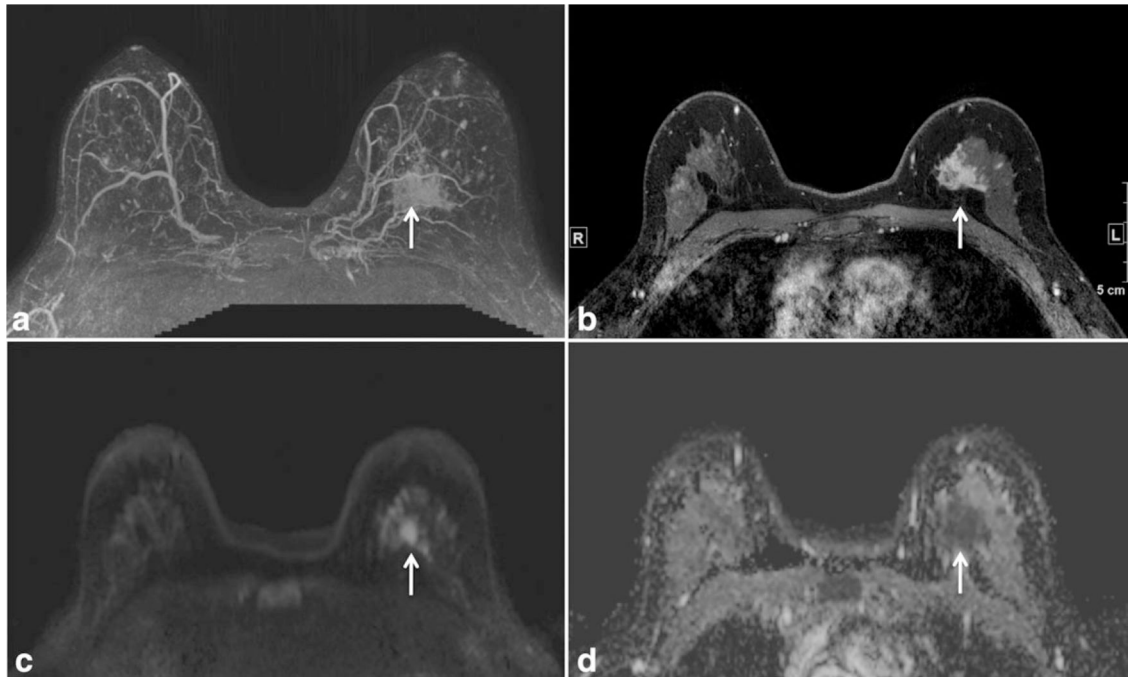


**Figure 12.**

Mammographically occult invasive lobular carcinoma in the left breast in a 44-year-old high-risk woman detected on a screening breast MRI with both dynamic contrast-enhanced breast and diffusion weighted breast MRI techniques. Maximum intensity projection image (a) and T1 contrast-enhanced image with fat suppression (b) demonstrate an irregular shaped mass with spiculated margins in the left breast (arrows). This mass is also readily detectable on diffusion weighted MRI (arrows), demonstrating high signal on the diffusion weighted image (c) and a low apparent diffusion coefficient (ADC) value on the ADC map (d).

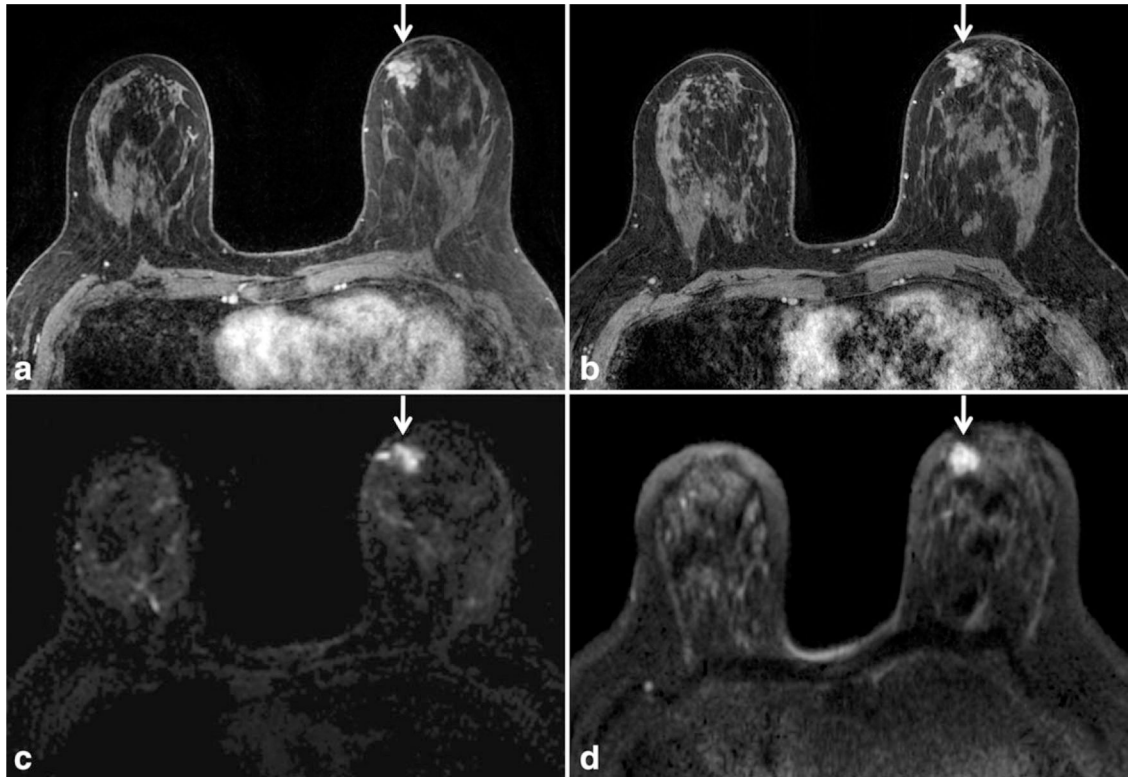


**Figure 13.**

Improved signal and spatial resolution on diffusion weighted MRI at 3T when compared with 1.5T in a patient newly diagnosed with DCIS (arrows). There is improved anatomic detail for both the reference postcontrast T1-weighted image with fat saturation at 3T (b) and the DWI image at 3T (d) when compared with respective images at 1.5T (a,c).

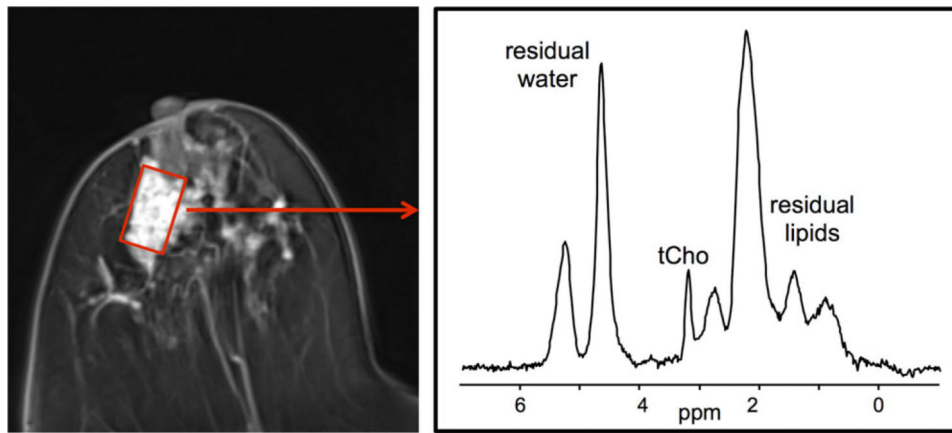


**Figure 14.** Single voxel breast MR spectra acquired at 3T in a patient with invasive breast cancer. The voxel was positioned within the enhancing lesion on the axial postcontrast T1-weighted images as indicated (red box). Corresponding spectra demonstrated a choline peak at 3.2 ppm. Figure courtesy of Patrick J. Bolan, PhD, University of Minnesota and Mark A. Rosen, MD, PhD, University of Pennsylvania.



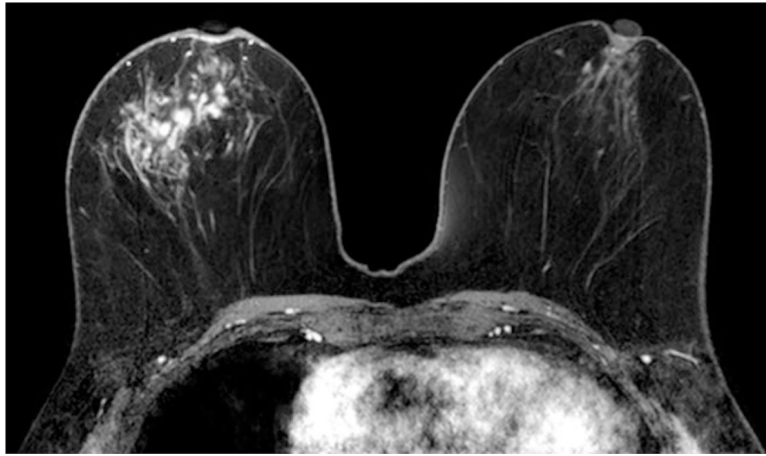


**Figure 15.**

Example breast MRI image using the University of Chicago protocol given in Table 2. This protocol obtains higher temporal resolution than the University of Washington DCE MRI protocol (1:17 min versus 2:51 min) at the expense of some spatial resolution (0.8 mm isotropic versus  $0.5 \times 0.5 \times 0.65$  mm). The example shown depicts a 76-year-old patient who underwent MRI for staging of newly diagnosed invasive breast cancer, which demonstrated a  $6.7 \times 4.8 \times 5.8$  cm region of segmental non-mass-like enhancement on DCE MRI. Image courtesy of Hiroyuki Abe, MD, PhD, University of Chicago.

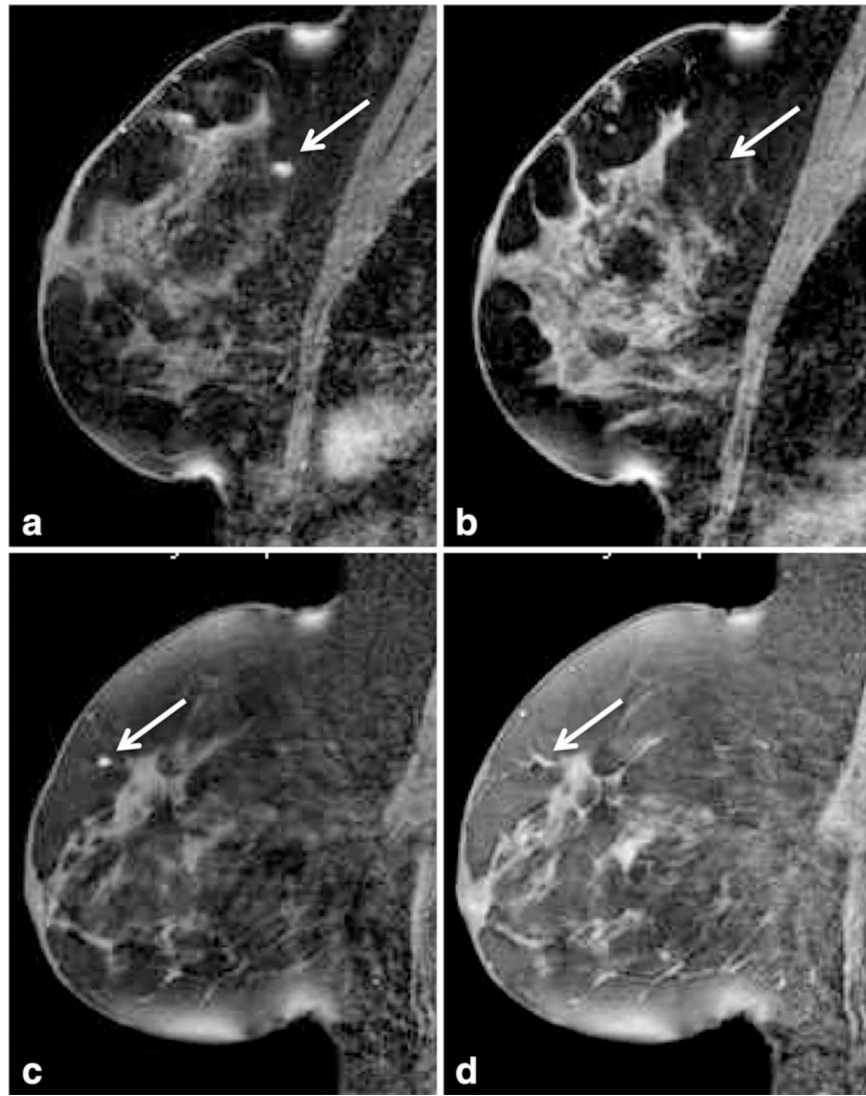


**Figure 16.**

Alteration of fat-suppression to improve visualization of obturator needle tip during MR guided biopsy. Sagittal T1-weighted images with fat suppression after administration of IV gadolinium are shown for two patients. In the first patient (top row), lesion identification scan (a) demonstrates excellent visualization of a 5 mm enhancing mass (arrow) at posterior depth in the superior breast surrounded by adipose tissue. Scan to confirm needle location before biopsy (b) demonstrates the challenge in identifying the obturator tip (arrow) with fat-suppression settings unaltered. In this case, the tip was identified to be within adipose tissue 5 mm superficial to the enhancing mass. In the second patient (bottom row), lesion identification scan demonstrates excellent visualization of a 3 mm enhancing focus (c) at anterior depth in the superior breast surrounded by adipose tissue. By decreasing the level of fat suppression for the needle-confirmation images (d) through alteration of the SPAIR delay, improved visualization of the obturator tip (arrow) was achieved and confirmed to be within the enhancing focus.

**Table 1**

## Potential Clinical Advantages of Breast MRI at 3T

Technical advantages	Potential clinical advantages
Higher spatial resolution	Improved anatomic/morphologic detail <ul style="list-style-type: none"> <li>—Better detection of small processes</li> <li>—More accurate assessment of lesion extent</li> <li>—Improved ability to resolve morphological features, such as fine spiculations and dark internal septations</li> </ul>
Higher temporal resolution	More accurate kinetic assessment <ul style="list-style-type: none"> <li>—Improved classification of peak and delayed enhancement</li> <li>—Ability to perform pharmacokinetic analysis</li> </ul>
Improved fat suppression	Increased lesion conspicuity
Improved contrast-to-noise ratio	Increased lesion conspicuity

Author Manuscript

Author Manuscript

Author Manuscript

Author Manuscript

**Table 2**

Technical Challenges of Breast MRI at 3T and Potential Solutions

Technical challenge	Practical clinical and imaging implications	Mitigating approaches
Increased specific absorption rate (SAR)	Tissue heating and patient comfort and safety	Parallel imaging with multichannel RF coils Alternate RF pulses (lower peak-amplitude) Sequence alterations: reduced flip angles, shorter echo train lengths, longer repetition times
Increased B <sub>0</sub> Inhomogeneity	Degradation of fat suppression and increased susceptibility artifacts	Multi-source parallel RF excitation Image-based shimming
Increased B <sub>1</sub> Inhomogeneity	“Tissue shading” or signal variability, reduced lesion conspicuity	Parallel imaging Multi-source parallel RF excitation 3D imaging techniques Higher flip angle

RF = radiofrequency.

Table 3

Comparison of Imaging Parameters for 1.5T and 3T Breast T1-Weighted DCE MRI Protocols

Field strength	1.5T (UW)	3T (UW)	3T (U Chicago)
Plane	Axial	Axial	Axial
Breast coil type	8 channel	16 channel	16 channel
Mode	3D	3D	3D
Sequence type	Fast gradient echo	Fast gradient echo	Fast gradient echo
Fat Suppression	SPAIR	SPAIR	SPAIR
Parallel imaging factor	1.5 R/L	2.7 R/L, 2.0 S/I	3 R/L, 2 S/I
TR (ms)	5.6	5.9	5
TE (ms)	3	3	2.5
Flip angle (degrees)	10	10	10
Field of view (cm <sup>2</sup> )	36 A/P × 36 R/L	22 A/P × 33 R/L	36 A/P × 36 R/L
Matrix	420 × 420	440 × 660	448 × 448
In-plane voxel size (mm)	0.85	0.5	0.80
Slice thickness (mm)	1.6	1.3 → 0.65 recon	1.6 → 0.8 recon
Scan time (min)	2:53	2:51	1:17

SPAIR = spectral presaturation by inversion recovery, SPAIR = spectral attenuated inversion recovery; S = superior; I = inferior; R = right; L = left; A = anterior; P = posterior.